Proceedings of CONF-FMCE 2026 Symposium: Smart City and Infrastructure Engineering
DOI: 10.54254/2755-2721/2026.CH38706

Two-Dimensional Perovskite Nanosheets: Synthesis and Advances in Solar Cell Applications

Xuanbo Shao

School of Materials Science and Engineering, Chongqing University, Chongqing, China
1076476721@qq.com

Abstract. Aiming at the prominent bottleneck of poor environmental stability for three-dimensional perovskite solar cells, two-dimensional (2D) perovskite nanosheets have attracted widespread research attention owing to their unique layered crystal configuration, excellent optoelectronic performance and intrinsically enhanced moisture-thermal stability. This paper firstly introduces three typical crystal phases (RP, DJ and ACI) of 2D perovskites and their tunable optoelectronic properties originating from quantum confinement effect. Then it summarizes four mainstream synthesis approaches including hot-injection, ligand-assisted reprecipitation, chemical vapor deposition and exfoliation, and discusses how experimental parameters modulate material morphology. Furthermore, its photovoltaic application strategies are elaborated, covering direct usage as light-absorbing layers, 2D/3D heterojunction interface engineering, as well as efficiency-stability coordinated optimization schemes. Finally, the existing challenges are analyzed, hoping to offer theoretical references for developing high-efficiency and long-lifespan perovskite photovoltaic devices.

Keywords: two-dimensional perovskite, nanosheets, synthetic methods, solar cells

1. Introduction

The ever-growing global energy demand, depletion of traditional fossil fuels, and environmental pollution and ecological damage induced by fossil-fuel combustion collectively drive the development of high-efficiency, clean and sustainable new-energy technologies, which constitute a core measure to advance the dual-carbon goal and realize socially sustainable development. As an abundant, zero-carbon-emission and readily accessible renewable energy resource, solar energy stands as a key research and industrial focus within the new-energy sector [1]. After decades of iterative development, photovoltaic technology has matured gradually and is becoming one of the primary alternatives to fossil fuels [2].

Among solar-cell technologies, the power-conversion efficiency (PCE) of crystalline-silicon solar cells is approaching the Shockley-Queisser theoretical limit. Consequently, perovskite solar cells (PSCs) have attracted intensive attention thanks to their high PCE and low fabrication costs [3]. Three-dimensional (3D) perovskites with distinctive structures and superior optoelectronic properties have emerged as a leading candidate material in this field. Nevertheless, 3D perovskites suffer from inferior stability under intense illumination and humid-hot conditions; they are prone to phase separation, interfacial-defect passivation failure and ion migration. Although perovskite solar

© 2026 The Authors. This is an open access article distributed under the terms of the Creative Commons Attribution License 4.0 (https://creativecommons.org/licenses/by/4.0/).

DOI: 10.54254/2755-2721/2026.CH38706

cells have pushed the PCE ceiling beyond the 26.7 % record of silicon cells to 34.6 %, their operational lifetime falls far short of the 25-year benchmark for silicon-based devices, severely hindering commercial deployment [4, 5]. Under such circumstances, developing novel perovskite materials that combine excellent optoelectronic performance and high stability has become a critical research breakthrough.

Compared with degradation-prone 3D perovskites, 2D perovskite nanosheets —core functional materials within the low-dimensional perovskite family — possess intrinsically enhanced stability. Large-volume hydrophobic organic cations are incorporated as interlayer spacers to build physical barriers against moisture invasion and suppress ion migration [6]. Such features substantially improve the thermal and moisture stability of materials and extend the service lifetime of corresponding photovoltaic devices. Meanwhile, 2D perovskites can directionally passivate coordinatively unsaturated defects in 3D perovskites and mitigate non-radiative recombination losses. Benefiting from their chemical inertness and compact layered stacking, they form protective barriers and synergistically boost carrier-transport efficiency and environmental stability of devices [7]. While optimizing PSC performance, 2D perovskite nanosheets feature facile, controllable multi-route fabrication compatible with low-cost, large-area industrial photovoltaic manufacturing. With balanced stability, optoelectronic merits and processing compatibility, they represent promising candidates for highly stable perovskite photovoltaics.

The application potential of 2D perovskite nanosheets has drawn widespread academic and industrial interest, with continuous advances in synthetic techniques, interface modification and device-architecture design. Accordingly, this paper reviews crystal structures and optoelectronic characteristics of 2D perovskite nanosheets, summarizes diverse synthetic protocols, and elaborates their deployment in research and industrialization of photovoltaic devices.

2. Crystal structures and optoelectronic properties of 2D perovskite nanosheets

2.1. Crystal structures of 2D perovskite nanosheets

Perovskite was first discovered in 1839 in metamorphic rocks of the Ural Mountains by Russian mineralogist Von Perovski and named after his surname. The archetypal perovskite, $CaTiO_3$, adopts an orthorhombic crystal system [8, 9]. Two-dimensional perovskites can be conceptually regarded as 3D ABX_3-type perovskite frameworks "cut" along specific crystallographic planes. In 3D perovskites, corner-sharing $[BX_6]^{4-}$ octahedra extend infinitely in three dimensions to construct continuous inorganic skeletons [10]. Upon introducing long-chain organic spacer cations, the three-dimensional connectivity of octahedra is disrupted, yielding finite-thickness inorganic slabs separated by organic interlayers and forming intrinsic quantum-well structures. In canonical 2D perovskites, corner-linked $[BX_6]^{4-}$ octahedra assemble into 2D inorganic sheets. Pioneering work by Mitzi demonstrated that long-chain organic ammonium cations (e.g., PEA^+, BA^+) act as structure-directing agents to template layered 2D architectures [11]. Spacer cations further modulate octahedral tilting and rotation patterns via hydrogen bonding, steric hindrance and van der Waals interactions.

DOI: 10.54254/2755-2721/2026.CH38706

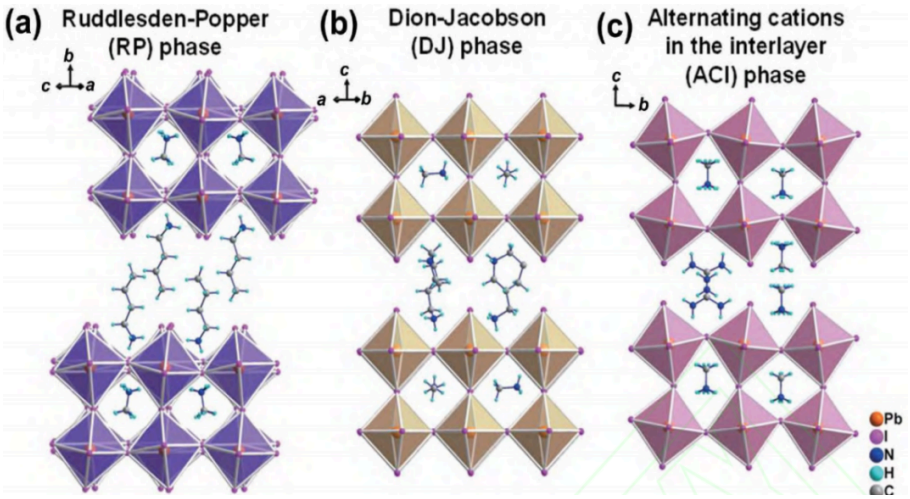


Figure 1. Two-dimensional perovskite crystal structures. (a~c) RP phase, DJ phase, and ACI phase [12]

Based on inorganic-layer offset modes and spacer-cation varieties, 2D perovskites are classified into three major structural families: Ruddlesden-Popper (RP), Dion-Jacobson (DJ), and Alternating Cations in the Interlayer Space (ACI) phases (Figure 1) [12]. The most extensively investigated RP phase follows the chemical formula $L_2A_{n-1}B_nX_{3n+1}$, where L denotes organic spacer cations, A small cavity-site cations within inorganic layers, B divalent metal cations, and X halide anions; n corresponds to the number of corner-connected octahedral sheets. In RP-phase structures, organic spacer cations adopt a bilayer arrangement between adjacent inorganic slabs, with interlayer coupling dominated by weak van-der-Waals forces. The DJ phase has the general formula $LA_{n-1}B_nX_{3n+1}$. Unlike RP phases, inorganic layers in DJ phases are perfectly aligned without in-plane displacement. Monolayer divalent diamine cations reside between inorganic sheets and establish quasi-covalent interlayer interactions, endowing DJ perovskites with superior structural stability and charge-transport capability relative to RP counterparts. The ACI phase lies intermediate between RP and DJ phases: A-site cations and GA-type spacer cations alternate within interlayer gaps accompanied by a (1/2, 0) in-plane displacement, delivering higher crystal symmetry than RP and DJ phases [12].

2.2. Optoelectronic properties of 2D perovskite nanosheets

Two-dimensional perovskite nanosheets constitute high-performance optoelectronic materials featuring tunable bandgaps, strong exciton effects, favorable carrier-transport behaviors and prominent nonlinear-optical responses. Their bandgap is thickness-dependent governed by quantum confinement, broadening as the octahedral-layer number n decreases [13]. For lead-iodide-based 2D perovskites, bandgaps can be continuously tuned from 1.83 eV (n = 5) to 2.43 eV (n = 1), enabling precise spectral modulation across the visible range. Insulating organic interlayers and nanoscale dimensionality synergistically amplify quantum and dielectric confinement, strengthening electron-hole coupling and yielding substantially larger exciton-binding energies than bulk 3D perovskites. Quasi-2D $CsPbBr_3$ nanosheets exhibit exciton-binding energies around 120 meV, while pure 2D perovskites reach 190–400 meV, stabilizing excitons at room temperature and facilitating efficient radiative recombination for outstanding luminescence performance. The photoluminescence quantum yield (PLQY) of $CsPbBr_3$ nanosheets peaks at 84.4 %, further improved to 98.4 % after

DOI: 10.54254/2755-2721/2026.CH38706

surface passivation, with an oscillator strength up to 1.18×10^4 exceeding conventional quantum-well materials [14-16]. In terms of carrier transport, 2D perovskite films achieve considerable mobilities; PEA_2PbI_4 attains a mobility of $8.0\ cm^2\ V^{-1}s^{-1}$. Nevertheless, inter-nanosheet hopping transport restricts long-range charge propagation. Surface functionalization with conjugated organic chromophores can enhance carrier yield by nearly one order of magnitude and extend carrier lifetimes to tens of microseconds. Furthermore, robust exciton effects grant 2D perovskite nanosheets large third-order nonlinear-optical coefficients and low saturation intensities. $CsPbBr_3$ nanosheets serve as saturable absorbers for passively Q-switched lasers with a modulation depth of 13.88 % and saturation intensity of $1.75\ MW\ cm^{-2}$. B-site doping with Cd^{2+}, Mn^{2+} and other ions further modulates linear and nonlinear optical properties, diversifying photonic-application avenue [17, 18].

3. Synthetic preparation of 2D perovskite nanosheets

3.1. Hot-injection method

Hot-injection represents one of the earliest protocols for colloidal-perovskite nanocrystal fabrication and has been extended to synthesize 2D nanosheets [19]. Typically, A-site cation precursors are rapidly injected at elevated temperatures (110–220 ℃) into high-boiling-point non-polar solvents containing metal halides (MX_2) and surface ligands such as oleic acid (OA) and oleylamine (OLA). Instant supersaturation triggers nucleation and crystal growth. Precise regulation over reaction temperature and duration is critical for tuning nanosheet thickness and lateral dimensions. Nanosheets generally form below 130 ℃, with thickness adjustable from monolayer to few-layer by varying temperature [20].

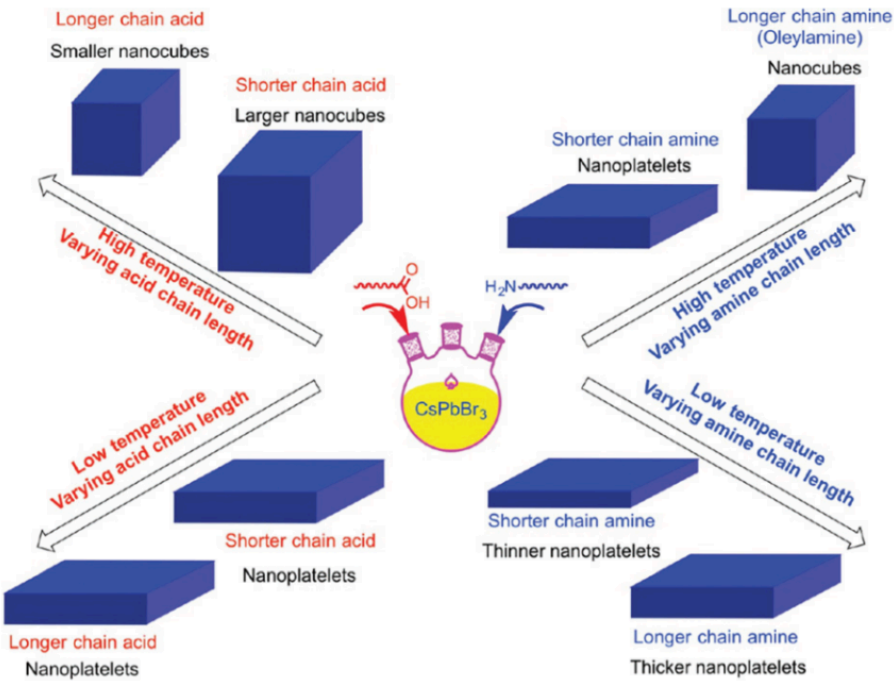


Figure 2. Effect of ligand chain length and reaction temperature on the morphology and size of halide perovskite nanocrystals prepared by the hot-injection method [21]

DOI: 10.54254/2755-2721/2026.CH38706

Pan and co-workers [21] explored how ligand-chain length and reaction temperature govern morphologies of $CsPbBr_3$ perovskite nanocrystals (Figure 2). At 170 ℃ hot-injection conditions, short-chain carboxylic acids (dodecanoic acid, octanoic acid, hexanoic acid) paired with long-chain oleylamine produce nanocubes. By contrast, combinations of long-chain oleic acid and short-chain amines (dodecylamine, octylamine, hexylamine) yield nanosheets irrespective of temperature. Reducing temperature to 140℃ and adopting C6- or C8-aliphatic amines enables accurate thickness control of nanosheets.

3.2. Ligand-assisted reprecipitation (LARP)

Ligand-assisted reprecipitation (LARP) is an important solution-based synthetic strategy widely adopted for preparing 2D perovskite nanosheets. This approach proceeds under ambient air at room temperature: perovskite-precursor salts or bulk crystals are dissolved in good solvents such as DMF or DMSO. Under vigorous stirring, the precursor solution is swiftly introduced into anti-solvents including toluene or hexane. Ligand-directed rapid precipitation generates nanocrystals [22]. Gupta et al. reported a modified LARP route to synthesize monodisperse oleic-acid and noctylammonium-bromide-capped $MAPbBr_3$ colloidal nanosheets at room temperature. The products possess lateral sizes of 17–20 nm, PLQY of approximately 50 %, and an optical bandgap of 2.3 eV; single-particle spectroscopy reveals multi-peak emission originating from quantum-confinement effects (Figure 3).

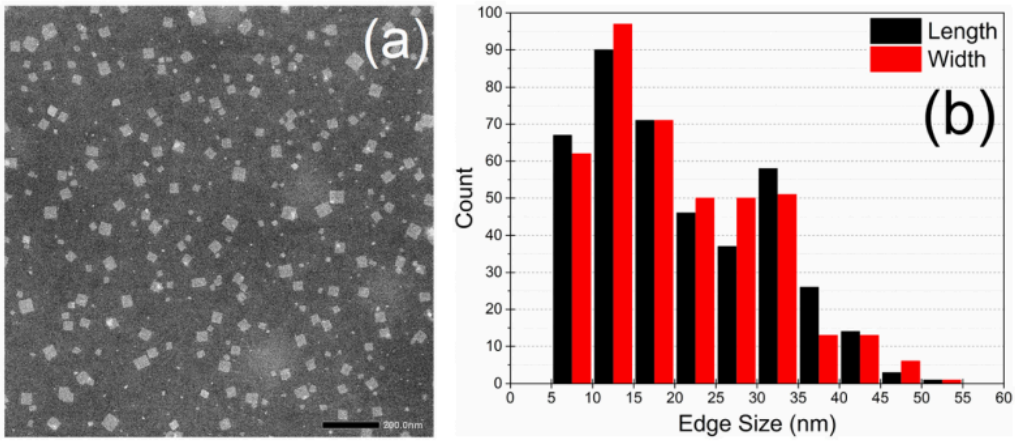


Figure 3. (a) Scanning transmission electron microscopy (STEM) image of MAPbBr3 nanosheets; (b) Particle size distribution histogram derived from the STEM image in (a) [23]

Nevertheless, LARP suffers challenges in precise dimensional control and obtaining narrow size distributions. Anti-solvent selection, synthesis temperature and ligand-chain length strongly influence product morphology and phase constitution. Even so, its operational simplicity and freedom from high-temperature/inert-atmosphere requirements render LARP attractive for large-scale manufacturing [23].

3.3. Chemical-vapor-deposition (CVD) method

Compared with solution-phase routes, chemical-vapor-deposition produces 2D perovskite nanostructures with superior crystallinity and diminished defect density, which is favorable for charge transport and optoelectronic-device performance [24]. Solvent-free CVD avoids grain-

DOI: 10.54254/2755-2721/2026.CH38706

boundary and surface-defect evolution. Multiple CVD workflows have been established for growing 2D organic-inorganic hybrid halide perovskites [24].

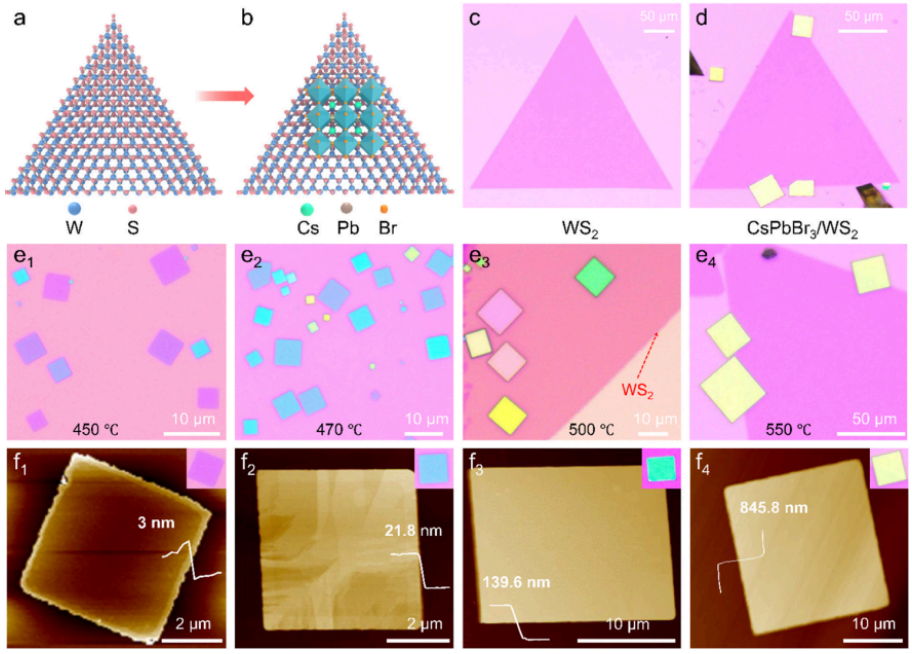


Figure 4. (a) Top view of the $CsPbBr_3$ crystal structure; (b) Top view of the $CsPbBr_3/WS_2$ heterostructure; (c) Optical microscope image of WS_2 nanosheets on a SiO_2/Si substrate; Optical microscope images (e1-e4) and atomic force microscope (AFM) images (f1-f4) of $CsPbBr_3/WS_2$ heterostructures prepared at different source temperatures [25]

Two-step CVD has been utilized for controllable epitaxial growth of $CsPbBr_3/WS_2$ vander-Waals heterostructures. Tuning growth temperature allows $CsPbBr_3$ nanosheet thickness to be reduced down to 3 nm (Figure 4) [25]. CVD facilitates large-area, epitaxial, selective and conformal growth [24]. However, high-equipment costs and stringent growth conditions limit its general applicability.

3.4. Exfoliation method

Foliation is a top-down fabrication strategy. Mechanical force or chemical treatment cleaves bulk layered perovskite crystals into atomically thin 2D nanosheets, subdivided into mechanical exfoliation and liquid-phase exfoliation. Mechanical exfoliation offers a straightforward pathway toward high-quality single-crystalline 2D perovskite flakes. Dhanabalan et al. solution-synthesized layered halide-perovskite microcrystals, then mechanically exfoliated them into ultrathin 2D sheets whose PLQY reached 42 %, considerably exceeding the 15 % of parent microcrystal aggregates [26]. Liquid-phase exfoliation employs sonication to disintegrate bulk layered perovskites, yielding ultrathin nanosheets approaching atomic thickness. The average PLQY rises from 15.2 % for bulk single crystals to 23.1 %, with maximum values hitting 39.61 %. Exfoliation preserves the outstanding crystallinity of bulk parent crystals to access ultrathin sheets, yet suffers relatively low yields, and lateral sizes are inherently constrained by the dimensions of starting bulk crystals.

DOI: 10.54254/2755-2721/2026.CH38706

4. Applications of 2D perovskites in solar cells

Thanks to excellent optoelectronic performance, 2D perovskite nanosheets exhibit promising prospects for solar-cell deployment. Incorporation of hydrophobic organic spacer cations imparts enhanced moisture, light and thermal stability, together with suppressed ion migration, making them a research highlight for PSCs [27]. Conversely, insulating organic interlayers within 2D perovskites induce large exciton-binding energies and anisotropic charge-transport behaviors, imposing performance constraints on devices [27]. Substantial progress toward reconciling efficiency and stability has been realized via material design, interface engineering and device-architecture optimization.

4.1. 2D perovskite nanosheets as light-absorbing layers

Drect employment of 2D perovskite nanosheets as light-harvesting layers represents their most straightforward photovoltaic application. Quasi-2D RP perovskites that combine high efficiency of 3D perovskites and enhanced stability of 2D systems have drawn major interest. Rational molecular design of organic spacer cations constitutes the core for boosting device performance. Nankai University researchers developed two semiconductor spacers, MeBThMA and CNBThMA. The donor-acceptor-structured CNBThMA features high dipole moments and ordered molecular stacking, mitigating organic-inorganic dielectric mismatch and improving charge-transport characteristics and film quality. RP-phase 2D perovskite solar cells adopting this spacer delivered a remarkable PCE of 20.82 %, setting a performance benchmark for devices with semiconductor spacers [28]. Additive engineering provides another effective optimization approach. Ginger's group at the University of Washington introduced combined NH4SCN and NH4Cl additives to optimize (PEA)2(MA)4Pb5I16 quasi-2D perovskite devices, achieving a stable PCE of 14.1 % at the time of publication [29].

4.2. 2D/3D heterojunctions and interface engineering

Constructing 3D/2D perovskite heterostructures has emerged as an effective methodology to simultaneously improve efficiency and stability of perovskite solar cells. In this strategy, a 2D-perovskite protective layer is built atop 3D perovskite absorbers. Hydrophobicity and defect-passivation capability of 2D materials shield bulk absorbers, while band-alignment engineering accelerates interfacial charge extraction. Zhou and co-workers reported a non-invasive surface-reaction strategy differing from conventional solution processing. Under controlled temperature-pressure conditions, cation surface diffusion triggers solid-state interfacial reactions to generate phase-pure, well-defined 2D-perovskite passivation layers [30], avoiding mixed-dimensional phase transitions commonly seen in solution-based approaches, and exhibiting universality toward diverse Ruddlesden-Popper molecules. N-i-p-architecture champion devices based on this technique achieved a PCE of 26.13 % (certified 25.66 %) without performance decay over 1200 h continuous operation, with a T_{50} lifetime of 1145 h. Mini-modules reached 23.03 % PCE with T_{80} = 1200 h. Uniform large-area films (10 cm × 10 cm) were demonstrated, manifesting good scaling potential.

Two-dimensional perovskite nanosheets can also be integrated into other functional positions within device stacks. Yang et al. blended 2D perovskite nanosheets with PMMA to fabricate down-conversion layers for bifacial semi-transparent solar cells. The composite simultaneously enables ultraviolet-photon down-conversion and interface passivation, restraining interfacial non-radiative

DOI: 10.54254/2755-2721/2026.CH38706

recombination. Devices retained more than 77 % of initial efficiency after 280 h UV aging. Bifacial devices adopting MoO_3/Au/MoO_3 transparent back-electrodes yielded PCEs of 14.26 % and 10.65 % for front-side and back-side illumination, respectively [30].

4.3. Synergistic optimization of efficiency and stability

A core dilemma persists for 2D perovskite solar cells: efficiency and stability are hard to reconcile. Low-n ($n \leq 3$) quasi-2D perovskites display excellent stability yet suffer poor charge-transport performance. To address this issue, researchers adopted tyrosine-mediated phase-modulation strategies. Hydrogen-bonding and cation-π dual-coordination stabilize low-n phases, regulate crystallization processes, elevate low-n-phase fractions and strengthen inter-layer electronic coupling, considerably extending carrier-diffusion lengths. Devices fabricated via this route attained a high PCE of 22.14 % with negligible hysteresis, alongside superior damp-heat stability, showing promise for large-area module manufacturing [27]. Additional modification tactics including dual-organic-spacer and A-site-cation co-regulation, and ethylenediamine-dihydroiodide phase modulation, enhance optoelectronic efficiency and operational stability for quasi-2D lead-based and tin-based perovskite solar cells, offering diverse technical pathways toward high-performance 2D-perovskite devices [31].

5. Conclusion

In summary, 2D perovskite nanosheets possess distinctive structures, outstanding optoelectronic properties and versatile synthetic routes, and have proven valuable and achieved remarkable advances for solar-cell applications. Through semiconductor-spacer design, additive engineering, 2D/3D-heterostructure construction and phase-modulation tactics, PCE values of 2D perovskite solar cells have risen from below 10 % in early studies to over 26 %, accompanied by major stability improvements. Nevertheless, preserving high efficiency upon scaling-up device dimensions and further suppressing non-radiative recombination remain key research priorities. With deepening understanding of crystallization kinetics, interfacial physics and device physics, commercial photovoltaic deployment of 2D perovskite nanosheets can be anticipated.

References

[1] Seyisi, T., Fouda-Mbanga, B. G., Mnyango, J. I., Nthwane, Y. B., Nyoni, B., Mhlanga, S., Hlangothi, S. P., & Tywabi-Ngeva, Z. (2025). Major challenges for commercialization of perovskite solar cells: A critical review. *Energy Reports, 13*, 1400–1415. https: //doi.org/10.1016/j.egyr.2025.01.019.

[2] Guerrero-Lemus, R., Vega, R., Kim, T., Kimm, A., & Shephard, L. E. (2016). Bifacial solar photovoltaics – A technology review. *Renewable and Sustainable Energy Reviews, 60*, 1533–1549. https: //doi.org/10.1016/j.rser.2016.03.041.

[3] Miller, O. D., Yablonovitch, E., & Kurtz, S. R. (2012). Strong internal and external luminescence as solar cells approach the Shockley-Queisser limit. *IEEE Journal of Photovoltaics, 2*, 303–311. https: //doi.org/10.1109/JPHOTOV.2012.2192103.

[4] Xiong, Z., Zhang, Q., Cai, K., Zhou, H., Song, Q., Han, Z., Kang, S., Li, Y., Jiang, Q., Zhang, X., & You, J. (2025). Homogenized chlorine distribution for > 27% power conversion efficiency in perovskite solar cells. *Science, 390*, 638–642. https: //doi.org/10.1126/science.ads0476.

[5] Li, N. X., Niu, X. X., Chen, Q., & Zhou, H. (2020). Towards commercialization: The operational stability of perovskite solar cells. *Chemical Society Reviews, 49*, 8235–8286. https: //doi.org/10.1039/D0CS00678A.

[6] Osada, M., & Sasaki, T. (2011). Two-dimensional dielectric nanosheets: Novel nanoelectronics from nanocrystal building blocks. *Advanced Materials, 24*, 210–228. https: //doi.org/10.1002/adma.201103413.

DOI: 10.54254/2755-2721/2026.CH38706

[7] Qi, X., Zhang, Y., Ou, Q., Ha, S. T., Qiu, C.-W., Zhang, H., Cheng, Y.-B., Xiong, Q., & Bao, Q. (2018). Photonics and optoelectronics of 2D metal-halide perovskites. *Small, 14*, 1800682. https: //doi.org/10.1002/smll.201800682.
[8] Galuskin, V. E., Gazeev, M. V., Armbruster, T., & Pertsev, A. (2015). Lakargiite $CaZrO_3$: A new mineral of the perovskite group from the North Caucasus, Kabardino-Balkaria, Russia. *American Mineralogist, 93*(11-12), 1903-1910. https: //doi.org/10.2138/am.2008.2900.
[9] Ji, D. H., Zhang, Y., Wang, S. L., & Liu, H. (2017). First principle study of the B-site ordered structure perovskite $BaFe_{0.5}Nb_{0.5}O_3$. *Journal of Hebei University (Natural Science Edition), 37*(6), 595-604.
[10] Wu, G. B., Liang, R., Ge, M. Z., & Chen, H. (2022). Surface passivation using 2D perovskites toward efficient and stable perovskite solar cells. *Advanced Materials, 34*(8), e2105635. https: //doi.org/10.1002/adma.202105635.
[11] Mitzi, D. B. (1999). Synthesis, structure, and properties of organic-inorganic perovskites and related materials. In K. D. Karlin (Ed.), *Progress in Inorganic Chemistry*. https: //doi.org/10.1002/9780470166499.ch1.
[12] Li, X., Hoffman, J. M., & Kanatzidis, M. G. (2021). The 2D halide perovskite rulebook: How spacer influences everything from the structure to optoelectronic device efficiency. *Chemical Reviews, 121*, 2230-2291. https: //doi.org/10.1021/acs.chemrev.0c01007.
[13] Wang, S. J., Chen, Z. Y., Zhang, G. F., & Li, Y. (2023). Quantum confinement effect on the electronic and optical properties of two-dimensional halide perovskites. *Computational Materials Science, 230*, 112524. https: //doi.org/10.1016/j.commatsci.2023.112524.
[14] Otero-Martínez, C., Ye, J., Sung, J., & Manna, L. (2022). Colloidal metal-halide perovskite nanoplatelets: Thickness-controlled synthesis, properties, and application in light-emitting diodes. *Advanced Materials, 34*(10), e2107105. https: //doi.org/10.1002/adma.202107105.
[15] Ran, L. X., Xiong, B. L., Wang, X. R., Zhang, N., Yang, S. C., & Liang, C. (2026). Photoelectric properties, synthesis and applications of two-dimensional perovskite nanosheets. *Science Bulletin, 1*-17. https: //link.cnki.net/urlid/11.1784.n.20260723.0954.002.
[16] Li, J., Luo, L. H., Huang, H. W., Ma, C., Ye, Z. Z., Zeng, J., & He, H. P. (2017). 2D behaviors of excitons in cesium lead halide perovskite nanoplatelets. *The Journal of Physical Chemistry Letters, 8*(6), 1161-1168. https: //doi.org/10.1021/acs.jpclett.7b00017.
[17] Wei, M. L., Zhang, H., Chen, M. Y., & Zhao, J. (2026). Optimizing luminescence in solution-processable 2D perovskite nanoplatelets: The role of Mn^{2+} doping and layer thickness. *Materials Research Bulletin, 194*, 113726. https: //doi.org/10.1016/j.materresbull.2025.113726.
[18] Litvin, A. P., Margaryan, I. V., Yin, W. X., Zhang, X. Y., Zheng, W. T., & Rogach, A. L. (2024). B-site doping of metal halide perovskite nanoplatelets influences their optical properties. *Advanced Optical Materials, 12*(8), 2301001. https: //doi.org/10.1002/adom.202301001.
[19] Choi, D., Kim, H., Bae, Y., Lim, S., & Park, T. (2024). Perovskite colloidal quantum dots with tailored properties: Synthesis strategies and photovoltaic applications. *ACS Energy Letters, 9*(6), 2633–2658. https: //doi.org/10.1021/acsenergylett.4c00632.
[20] Otero-Martínez, C., García-Lojo, D., Pastoriza-Santos, I., Pérez-Juste, J., & Polavarapu, L. (2021). Large-scale colloidal synthesis of two-dimensional halide perovskite nanoplatelets. *Angewandte Chemie International Edition*. https: //doi.org/10.1002/anie.202109308.
[21] Pan, A. Z., He, B., Fan, X. Y., Liu, Z. K., Urban, J. J., Alivisatos, A. P., He, L., & Liu, Y. (2016). Insight into the ligand-mediated synthesis of colloidal $CsPbBr_3$ perovskite nanocrystals: The role of organic acid, base, and cesium precursors. *ACS Nano, 10*(8), 7943–7954. https: //doi.org/10.1021/acsnano.6b03863.
[22] Abarbanel, O., Hirzalla, R., Aridor, L., Michman, E., & Hadar, I. (2025). Studying the effect of dimensions and spacer ligands on the optical properties of 2D lead iodide perovskites. *Nanoscale, 17*(12), 7153–7163. https: //doi.org/10.1039/d4nr05516k.
[23] Gupta, S., Vorontsov, D., Fučíková, A., Trojánek, F., Zákutná, D., Veselý, J., Harcuba, P., & Dopita, M. (2026). Multi-peak single object emission of $MAPbBr_3$ nanoplatelets synthesised using a non-template ligand-assisted reprecipitation route. *Nanoscale, 18*, 3209–3219. https: //doi.org/10.1039/d5nr04000k.
[24] Kang, K., Kang, M., Cho, H., Ham, A., & Kim, T. S. (2021). Strategies for chemical vapor deposition of two-dimensional organic-inorganic halide perovskites. *iScience, 24*, 103486. https: //doi.org/10.1016/j.isci.2021.103486.
[25] Lin, X. H., Chu, A. S., Chen, L., Zhang, T. C., He, C. L., Huangfu, Y., Li, W., Zhang, Z. C., Kang, T., & Duan, X. D. (2026). Controlled epitaxy of perovskite van der Waals heterostructures enables advanced self-powered broadband photodetectors. *Nano Today, 67*, 102976. https: //doi.org/10.1016/j.nantod.2026.102976.
[26] Dhanabalan, B., Castelli, A., Palei, M., Spirito, D., Manna, L., Krahne, R., & Arciniegas, M. (2019). Simple fabrication of layered halide perovskite platelets and enhanced photoluminescence from mechanically exfoliated flakes. *Nanoscale, 11*, 8334–8342. https: //doi.org/10.1039/c9nr00638a.

DOI: 10.54254/2755-2721/2026.CH38706

[27] Yang, Y., Hoang, M. T., Chiu, W.-H., Yu, Y., & Wang, H. (2024). Efficient bifacial semitransparent perovskite solar cells using down-conversion 2D perovskite nanoplatelets-poly(methyl methacrylate) composite film. *Small Structures, 5*(6), 2300547. https: //doi.org/10.1002/sstr.202300547.

[28] Dong, X., Zhang, H., Li, J., Yang, L., Ma, Y., Liu, H., Hu, Z., & Liu, Y. (2025). Semiconductor spacer with donor-acceptor structure drives 2D Ruddlesden–Popper perovskite solar cells beyond 20% efficiency. *Angewandte Chemie International Edition, 64*(22), e202501210. https: //doi.org/10.1002/anie.202501210.

[29] Fu, W., Wang, J., Zuo, L., Gao, K., Liu, F., Ginger, D., & Jen, A. K.-Y. (2018). Two-dimensional perovskite solar cells with 14.1% power conversion efficiency and 0.68% external radiative efficiency. *ACS Energy Letters, 3*(9), 2086–2093. https: //doi.org/10.1021/acsenergylett.8b01181.

[30] Zhang, K., Wang, Y., Guo, L., Tao, M., Guo, H., Zhang, X., Song, Z., Wen, J., Yang, Y., Shao, J., Zhou, H., & Song, Y. (2025). Surface diffusion engineering of a 2D perovskite layer for efficient perovskite photovoltaics. *Nature Synthesis, 4*, 1386–1395. https: //doi.org/10.1038/s44160-025-00865-w.

[31] Peng, S., Liu, J., Liang, C., Chen, G., Shi, Y., Miao, Z., Liang, W., Zhang, T., Xie, Y., Zhang, Y., Song, Y., & Li, P. (2025). Achieving low n value phases and unobstructed carrier transport toward high performance quasi 2D perovskite solar cells and modules. *Joule, 9*(9), 102079. https: //doi.org/10.1016/j.joule.2025.102079.